Evaluation of Radiometric Calibration Accuracy of GOES Imager Infrared Data Using GSICS GEO-LEO Data

Fangfang Yu[1], Xiangqian Wu[2], M.K. Rama Varma Raja[3], Likun Wang[4], Yaping Li[3], and Mitch Goldberg[2]

1: ERT Inc. @ NOAA/NESDIS/STAR e-mail: Fangfang.Yu@noaa.gov; 2: NOAA/NESDIS/STAR; 3. IMSG @ NOAA/NESDIS/STAR; 4. Dell @ NOAA/NESDIS/STAR

Abstract

The Geostationary Operational Environmental Satellite (GOES) mission consists of a series of three-axis body-stablized geosynchronous satellites operated by National Oceanic and Atmospheric Admistration (NOAA) that provide continuous stream of data covering the United States and its neighbring environs. Two significant issues associated with the three-axis stablized platforms were recognized in the process of onboard calibration for the infrared data: extraneous heating of the instruments around satellite midnight time, and the changes of scan mirror emissivity with incoming radiation at east-west scan direction. In operation, the Midnight Blackbody Calibration Correction (MBCC) method based on the relationship between day-time calibration data and telemetry temperature was developed to empirically compensate for the errorreous instrument responsivity near midnight. The variation in scan mirror emissivities was corrected with a set of fixed angle-dependent correction coefficients derived from full-disk scan space view data. However, uncertaity remains with MBCC calibration accuracy and the scan angle calibration residuals. The objective of this study is to investigate the impact of the MBCC on the diurnal calibration accuracy of the GOES-11 and -12 Imager infrared (IR) channels, as well as to examine the scan-mirror emissivity calibration residuals using collocation data generated by the Global Space based Inter-Calibration System (GSICS) baseline algorithm. Using two new generation hypespectral instruments onboard low-earth orbital (LEO) satellites as references, the results of this study show that most IR channels, especially the long-wave channels, have apparent diurnal calibration variations. The MBCC method, once implemented, can reduce the diurnal calibration variation except for Ch4(10.7μm) on both GOES-11/12 Imagers. Analysis of the GOES with IASI night-time collocation data (before 10:00pm) indicates that scan-angle calibration residual at each IR channel is very small with uncertainty less than 0.1K. The day-time collocation data may be affected with the anisotropic reflectance/emissivity of the collocated scenes. Our results suggest that either night-time GOES vs. IASI collocation data (taken before the midnight calibration anomaly) or daytime collocated scenes taken nadir/near nadir should be used to generate the GSICS GEO-LEO correction coefficients to improve the calibration accuracy of the operational GOES Imager instruments.

1. Introdcution

The Geostationary Operational Environmental Satellite (GOES) is a series of three-axis body-stablized geosynchronous satellites operated by National Oceanic and Atmospheric

Administration (NOAA) of the United States (US). Located at 75°W (GOES-East) and 135°W(GOES-West) about 35,800km above the Equator, two GOES satellites are normally operated simultaneously to provide continuous streams of satellite data for weather monitoring and forecasting operations of the U.S. and its neighbouring environs. The resulting quantitative meteorological products, such as atmospheric temperature and moisture profiles, winds, and precipitation are important inputs to the numerical weather prediction (NWP) systems and the global climate change studies. With the increasingly demanding requirements from more accurate weather nowcasting models and climate change studies, it is essential to continually improve the operational GOES satellite data stream.

Compared to the spinning geostationary (GEO) satellites which spends over 90% of their time scanning space, these three-axis stablized GOES Imager and Sounder instruments always observe the Earth except for some brief routine disruptions to view space and blackbody for onboard calibration purposes (Weinreb et al. 1997). However, around the satellite midnight time when the instrument faces the Sun, the three-axis stabilized instruments undergo significant heating followed by subsequent cooling (Johnson and Weinreb 1996, Yu and Wu 2010). During this period, the non-perfect GOES blackbodies reflect background fluxes emitted from the surrounding compoenents, causing errors in instrument responsivity (Johnson and Weinreb 1996). To reduce the midnight calibration errors, the midnight blackbody calibration correction (MBCC) which is based on the empirical relationship of the day-time calibration slopes and primary telescope temperature data was developed to replace the operational calibration algorithm when necessary (Johnson and Weinreb 1996). Another issue with the three-axis stabilized satellite is the varying scan mirror emissivity. The GOES scan mirror is coated with absorptive silicon-oxide. As a result, the mirror emissivities varies with the incidence angle of the incoming radiation from the viewed scene. In operation, the east-west scan angle dependent scan mirror emissivity is corrected with a set of fixed coefficients generated with the space-view counts from one-day full-disk scans above the North Pole (Weinreb et al. 1997). However, recent analysis of GOES Imager infrared (IR) data with different well-calibrated instruments onboard low-earth orbital (LEO) satellites reveals that large brightness temperature (Tb) biases still exist at the long-wave channels around satellite midnight time (Mittaz and Harris 2008, Rama V.R. et al. 2009). Since MBCC is implemented on an as-needed basis, it remains uncertain precisely how it impacts GOES diurnal calibration variation. To to our knowlesge, no independent evaluation has been conducted to examine scan-angle dependent calibration residuals. Additionally, evaluations of current GOES operational calibration accuracy are helpful in any case to reduce the potential calibration errors for GOES-R, which is scheduled to launch in 2015.

Cross-sensor inter-calibration has proved to be a powerful tool to evaluate instrument calibration peformance and to identify and diagnose calibration anormalies. By comparing the collocated nadir pixels within a certain brief orbital intersection period, the simulatenous nadir overpass (SNO) method has been widely used to evaluate the calibration accuracy of LEO instruments with similar spectral response functions (SRF) in the polar regions (Cao et al. 2004). The ray-matching technique is another common inter-calibration techique, especially for the visible channels on the GEO satellites. It uses spatially collocated but nearly coincident and co-angled pixel radiance in nadir and near nadir areas to transfer the reference LEO satellite's calibration accuracy to a GEO or another LEO satellite (Doelling et al. 2004, Wu and Sun 2005).

Recently, near simultaneous nadir observations were used to examine the calibration accuracy of GOES Imager IR instruments by inter-comparison of GEO data with those from the new generation of hyperspectral instruments onboard the polar-orbitting satellites (Gunshor et al. 2009, Wang et al. 2009). However, these studies were based on an average of a certain period with near-nadir collocation data in tropical regions. The overall evaluation may average down or canceal out the subtle calirbation variation of GOES earth-observation sensors.

The Global Space based Inter-Calibration System (GSICS) GEO-LEO baseline inter-calibration algorithm provides a unique opportunity to examine the GOES Imager calibration system over a variety of temporal scales and viewing conditions. As a critical space componenet of the Global Earth Observation System of Systems (GEOSS), the GSICS project aims to improve the calibration accuracy of the operational instruments and provide consistently calibrated data for NWP and climate monitoring by inter-calibration of a diverse range of satellite data (Goldberg 2007). Currently, the GSICS GEO-LEO inter-calibration uses two hyperspectral instruments, the Atmospheric Infrared Sounder (AIRS) om the NASA Aqua satellite and the Infrared Atmospheric Sounding Interferometer (IASI) on the EUMETSAT Metop-A satellite, as calibration standards to correct the GEO IR data (Wu et al. 2009). Since spring 2009, NOAA has been routinely generating GEO-LEO collocation data to provide correction coefficients to improve the calibration accuracy of the operational GOES instruments (Yu et al. 2009).

The objective of this paper is to evaluate the GOES calibration accuracy associated with three-axis stablized platforms using the collocation data generated with the GSICS GEO-LEO baseline algorithm, specifically the impact of MBCC on the GOES Imager diurnal calibration accuracy and the scan angle calibration residuals associated with two GOES satellites: GOES-11 (GOES-West) and GOES-12 (GOES-East). The paper is organized as follows: Section 2 describes the calibration systems of the GOES Imager and hyperspectral AIRS and IASI instruments, and the GSICS GEO-LEO inter-calibration baseline algorithm. Section 3 introduces the data and methodology used in this study and clarifies the selection of homogeneous collocation data to ensure reliable results. Section 4 presents the diurnal calibration variationa and scan-angle dependent calibration residuala for each GOES-11/12 Imager IR channel. Section 5 provides the conclusions of this study.

2. Instruments

2.1 GOES Imager

Each GOES Imager has five-channel imaging radiometor, including one visible (Ch1) and four IR channels (Ch2, Ch3, Ch4, Ch5 or Ch6) to sense solar reflected or emitted energy from sampled areas of the Earth (ITT GOES Data book). The Imagers on GOES-11 and GOES-12 have a total of 7 square detectors for the IR channels, including two InSb(Indium Antinomide) detectors for Ch2 (3.9μm) and five HgCdTe (Mercury Cadmium Telluride) detectors for the other three channels(Table 1). GOES-11 has one detector for Ch3 (6.5μm, water vapor channel), and two detectors for Ch4(10.7μm) and Ch5(12.0μm). GOES-12 updated GOES-11 design by replacing the two detectors ofor Ch5(12.0μm) with one detector for Ch6 (13.3μm, CO_2

absorption channel). Additionally, the detector for the water vapor channel was replaced with two narrow-band units(Figure 1). Each detector for the two-detector IR channels has an instantaneous geometric field of view (IGFOV) of 112 μrad, resulting in a subsatellite pixel of 4km per side. The detectors for the one-detector channels have an IGFOV of 224 μrad with subsatellite pixels of 8km per side. During imaging operations, a scan line is generated by sampling the detector signals while the the scan mirror rotates in the east-to-west (E-W) direction. The combination of scan rate and detector sample rate deminates that each IR sample in the E-W direction spans 64 μrad, resulting in an about an E-W oversampling of 75% for the Imager data (Menzel and Purdom 1994). The GOES IR specification of calibration accuracy is ≤1K for each IR channel (GOES Imager data-book).

The GOES onboard infrared (IR) radiance is calibrated using the non-linear combination of the data from viewings of the onboard blackbody (BB) and space (SP) (Weinreb et al. 1997). The operational calibration algorithm accounts for the variation of scan mirror emissivities in the E-W direction. The operational calibration equation can be written as:

$$[1-\varepsilon(\theta)]R + \varepsilon(\theta)R_M = qX^2 + mX + b \qquad (1)$$

where $\varepsilon(\theta)$ is the scan mirror emissivity at scan angle θ. The maximum scan angle of GOES Imager is about 10^o ($\theta<10^o$). R is the scene radiance, R_M is the radiance of the scan mirror, and X is the earth scene output in raw count. The q, m and b are the calibration coefficients. In operation, the correction of scan angle dependent emissivity is carried out using the space lines in the full-disk scan scenes. A daily average profile of emissivity (ε) versus scan angle (θ) was computed as the average over all hours within the specific day and then stored in a database on the ground-system computer. The second-order coefficient (q) is determined from pre-launch data and assumed fixed over the instrumet mission life. The first-order slope (m) and intercept b values are calculated on-orbit, determined with the instrument BB and SP data . Since Imager conducts BB measurements every 30 minutes, the slope (m) value is updated after every BB view and can be derived as followed:

$$m = [r_{bb} - q(X_{bb}^2 - X_{sp}^2)]/(X_{bb} - X_{sp}) \qquad (2)$$

where the variables with sp and bb are same as in Equation (1) for the space look and blackbody measurements. The intercept (b) is derived from Equations (1) and (2) and updated after every space clamp event which occurs at a frequency of 2.2 or 36.6 seconds with the correction of the 1/f noise (Weinreb et al. 1997).

This calibration algorithm does not account for any change of emitted flux from the surrounding environment. However, the non-perfect GOES Imager BB can reflect the changing background flux to the detectors around midnight time when the instrument experiences heating, which causes erroneous instrument responsivity for about eight hours centered on satellite midnight (Johnson and Weinreb 1996). It was found that the midnight calibration error is strongest at shortwave channel and decreases with increasing wavelenght. To modify the midnight calibration anomaly, the midnight blackbody calibration correction (MBCC) was develped based on the regression between the normal calibration slopes from Equation (2) and the temperature of Imager optics components (Weinreb and Han 2003). The primary telescope mirror temperature seems to be the best predictor to the calibration coefficient at time beyond the

eight hours of midnight effect. When the calibration slopes from the normal calibration algorithm (Equation 3) deviate from the values calculated from the emperical linear relation at a certain threshold, MBCC is set to replace the operational calibration slopes (John and Weinreb 1996). The MBCC cab be switched on or off directly and is applied in addition to other calibration enhancements.

Table 1. GOES, AIRS and IASI instrument details.

GEO	**Nadir Longitude**	**IR spectral range**	**IGFOV at nadir (km)**	**Applications**	**Specification**
GOES-11 Imager	135°W	Ch2:3.78-4.03μm	4	Nighttime cloud	≤1K
		Ch3:6.47-7.04μm	8	Water vapor	
		Ch4:10.23-11.25μm	4	Sea surface temperature and water vapor	
		Ch5:11.58-12.50μm	4		
GOES-12/13 Imager	75°W	Ch2:3.76-4.03μm	4	Night time cloud	
		Ch3:5.77-7.34μm	4	Water vapor	
		Ch4:10.23-11.24μm	4	Sea surface temperature and water vapor	
		Ch6:12.96-13.72μm	8	Cloud cover and height	

LEO	**IR spectral range**	**IGFOV at nadir (km)**	**Equator ascending local time**	**Specification**
Aqua AIRS	2378 IR bands: 3.74 - 4.61μm, 6.20 - 8.22μm, and 8.80 - 15.4μm	13.5	1:30pm	<0.2K@256K
Metop-A IASI	8462 bands from 3.63-15.5μm	12	9:30pm	<0.5K@280K

*: NedT@300K for Ch2,4,5, and 6, @230K for Ch3 (water vapor channel)

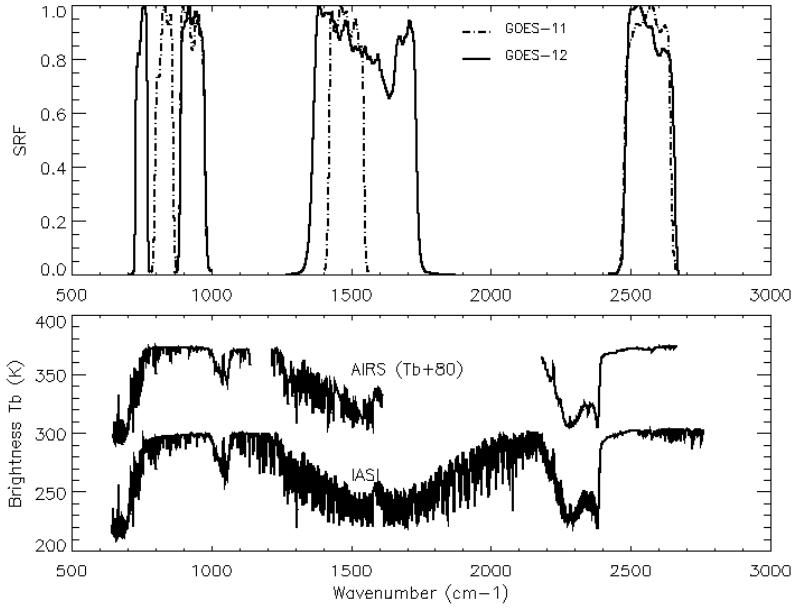

Figure 1. Spectral response functions of GOES-11/12 Imager IR channels and the AIRS and IASI spectra over the cloudess tropical atmosphere simulated with the line-by-line radiative transfer model (LBLRTM). The AIRS brightness temperature plus 80K is plotted for graphical purposes.

2.2 AIRS

AIRS is a hyper-spectral grating IR spectrometer onboard the National Aeronautics and Space Administration (NASA) Aqua satellite which ascends the Equator at approximately 1:30pm every day. AIRS measures the thermal infrared spectra onto 17 linear arrays of HgCdTe detectors on a focal plane with 2378 IR channels covering the bands of 3.75-4.59μm (2181-2665 cm^{-1}), 6.20-8.22μm (1217-1614cm^{-1}), and 8.8-15.4μm(650-1136cm^{-1}) (Auman et al. 2003, Figure 1). AIRS provides ±49.5° ground coverage through a cross-track rotary scan mirror to obtain 90 footprints in 2.017s at every scan line (Pagano et al. 2003). Assuming a circular FOV of 1.1^{o}, the corresponding nadir footprint is 13.5km in diameter.

The AIRS instrument has high spectral and radiometric calibration accuracy to meet the requirements of studies on climate and other environmental changes. The specification of absolute radiometric calibration accuracy requirement is 3% in radiance with spectral resolving power ($\lambda/\Delta\lambda$) of 1200. AIRS relies on accurate measurements of its deep space view (cold reference) and an on-board calibrator BB (warm reference) for radiometric calibration. It applies the Mueller Matrix in a radiometric transfer equation to correct the absorptive and polarized effects of the scan mirror. After over 7 years in orbit, it has been found that both the spectral and radiometric calibration accuracies are within the (Pagano et al. 2009).

2.3 IASI

IASI is a thermal infrared sounder onboard the European Metop satellite with a 9:30 AM equator descending mode. The Michelson interferometer is operated in the 3.6μm – 15.5μm ($2760cm^{-1}$ – $645cm^{-1}$) spectral range at 8264 channels with a 0.25 cm^{-1} spectral sampling interval. (Blumstein et al. 2004). The IASI earth view observations are obtained by a step scanning mirror covering with a ± 47.85° range in 30 scan steps at every scan cycle. At each step, the field of regard (FOR) includes 2x2 1.25° circular FOVs with a pixel resolution of 12 km at nadir. Like GOES and AIRS, IASI also depends on the space view and BB data as cold and warm reference measurements. The calibration specification for IASI calibration is 0.2K at 3-sigma, allowing for temperature and humidity profiles with a vertical resolution of one kilometer and an average accuracy of 1K and 10%, respectively (Blumstein et al. 2007). Analyses of the in-flight IASI data indicate that IASI has operated well within these specifications of radiometric calibration accuracy since being placed in orbit (Blumstein et al. 2009). Due to its spectral consistency and high-quality radiometric calibration, IASI measurements are used to inter-calibrate the radiometric calibration accuracy of broad-band instruments (Hewison and Konig 2008, Wang et al. 2009).

2.4 Radiometric calibration difference between AIRS and IASI instruments

The studies of inter-calibration of AIRS and IASI data using SNO observations and the double differences method indicate that there is very small radiometric calibration difference between in these two hyperspectral instruments (Tobin et al., 2008, Strow et al. 2008). Using the JMA (Japan Meteorological Agency)'s gap filling method to compensate for the AIRS missing channels, Wang et al. (2010) found that the calibration difference between AIRS and IASI data over the GOES IR spectra is less than 0.1K with 95% confidence with AIRS slightly warmer than IASI. No apparent diurnal calibration variation was found for either AIRS or IASI data (Elloit et al. 2009). The fixed scan angle of the AIRS instrument, as well as the correction of absorption and polarization of the scan mirror, makes it unlikely have scan angle dependent calibration uncertainty. Thus, this instrument can be used to evaluate the scan angle effect of other instruments (Tobin et al. 2006). Recent inter-comparisons of AIRS and IASI data at varying scan angles at Dome C show consistent Tb biases between AIRS and IASI except for a slight asymmetric discrepancy in a long-wave IR window channel when the scan angle is larger than 40^o (Elloit et al. 2010.) The root cause of this discrepancy is not very clear as yet.

3. Data and Methods

3.1 GSICS GEO-LEO Baseline Collocation Data

The success of inter-calibrations that are across different orbits largely depends on the accurate identification of collocations for the targets. Four criteria, including spatial collocation, temporary concurrency, viewing geometry matching, and spectral transformation are applied to generate the collocation data in the GSICS GEO-LEO inter-calibration baseline algorithm (Wu et al. 2009 and Hewison 2010). The spatial collocation threshold is defined as the nominal radius

of the LEO FOV at nadir (13.5km for AIRS and 12km for IASI). An array of 5x3 GOES pixels (about 12km x 12km accounting for GOES east-west oversampling effect), centered at the GEO pixel which is closest to the center of LEO FOV, is treated as a LEO spatially collocated pseudo GEO pixel ($FOV_{collocation}$). In the baseline algorithm, another co-centered target area with 17x9 (3x3 LEO FOV for GOES east-west oversampling) GEO pixels is also used to characterize the spatial uniformity in the environment of the collocation scenes ($ENV_{collocation}$).

To ensure the selected collocated pixels have been observed under comparable conditions, a threshold of 1% difference in the secant of the viewing geometry alignment of zenith angle is applied in the baseline algorithm to limit the difference of the optical path length between the two measurements. With this viewing zenith threshold, the angle difference reduces with increasing zenith angle, with a 1% difference near nadir and 0.5% at zenith angle (Wu et al. 2009, Wang et al. 2010). The time difference between the GEO and LEO observations at the collocated scenes should be less than 5 minutes, which is about the time for an inhomogeneous feature, if exists, to move across a collocation scene ($FOV_{collocation}$) at typical wind speeds (Wu and Sun 2004).

After spatial and temporal collocation and alignment of viewing geometry, the hyperspectral channels are convoluted with the GEO SRF to simulate GEO's broadband radiance. The synthetic radiances in the pseudo-channels are generated using the following equation:

$$R_{GEO} = \frac{\int_{\upsilon} R_{\upsilon} \Phi_{\upsilon} d\upsilon}{\int_{\upsilon} \Phi_{\upsilon} d\upsilon} \qquad (3)$$

where R_{GEO} is the simulated GEO radiance, R_{υ} is LEO radiance at wavenumber υ, and Φ_{υ} is GEO spectral response at wavenumber υ. However, as shown in Figure 1, AIRS does not provide complete spectral coverage of the GEO channels either by design or for some poorly performing channels. The JMA's gap filling method, which compensates for the missing hyper-spectral channels by regression with eight atmospheric model profiles is used to account for the radiances in these gap and bad channels (Tahara and Kato 2008).

Figure 2 displays one day spatial distributions and temperature ranges of GOES-11/12 vs. IASI collocation data for Ch4 (10.7μm) on June 9, 2009. Most of the GOES-11 collocation data are situated over the Pacific Ocean. Meanwhile, GOES-12 has large amounts of collocation data over North and South America. It clearly shows that the baseline collocation data cover large temperature and spatial coverage ranges with multiple LEO orbital locations. The wide geographical locations and long time duration provide a unique opportunity to investigate the GOES diurnal calibration accuracy and scan angle calibration residuals.

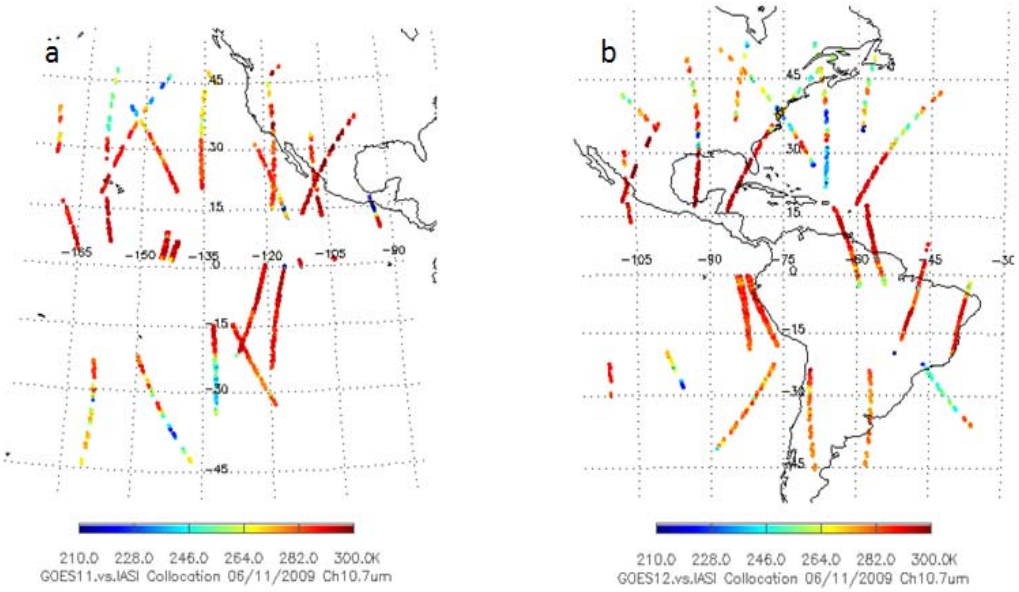

Figure 2. An example of spatial distributions and temperature ranges of GOES vs. IASI collocation on June 11, 2009 for GOES-11 (a) and GOES-12 (b), respectively.

3.2. Selection of homogeneous scenes

In order to compensate for the possible navigation errors and differences in module transfer functions for the different satellite instruments, homogeneous collocation scenes are often used in satellite inter-calibration to ensure that the instruments measure the same earth targets. In this study, a homogeneous collocation is identified when the standard deviations of GOES pixel brightness temperature (Tb) are less then 1.0K within both $FOV_{collocation}$ and $ENV_{collocation}$ areas.

$$STDV(Tb_{fov}) < 1.0 \text{ and } STDV(Tb_{env}) < 1.0 \qquad (4)$$

Although radiance is proportional to the energy received at the sensor, due to the nonlinear relationship between the radiance and brightness temperature, a fixed radiance-based threshold becomes stricter as scene temperature decreases within each IR channel. This might result in a warm-biased Tb difference. As there are fewer cold collocation scenes than warm ones at the daily collocation data (Figure 1), this Tb-based threshold can provide more opportunities for the cold collocation scenes to pass the homogenity filters and thus ensure a wide temperature range for the all-sky GEO-LEO inter-calibration.

Note that the baseline algorithm does not apply any threshold for the azimuth angle alignment to identify collocation data, recognizing that day-time thermal emission for the infrared window channels may be anisotropic over land surface due to the differential heating of the surface as a result of shadowing (Minnis et al. 2004). As GOES-12 has large amount of

collocations over land (Figure 2b), a threshold to reduce the uncertainty with the azimuth angle alignment is added to the day-time homogeneous selection for both GOES-11 and -12 data:

$$\left|AZI_{geo} - AZI_{leo}\right| < 60^{o} \qquad (5)$$

where AZI_{geo} and AZI_{leo} are the azimuth angle for the GOES and LEO (AIRS or IASI) instruments at the homogeneous collocation scenes.

3.3. Tb bias at the collocation scenes

Everyday there are tens to hundreds of collocation scenes passing the homogeneity filters of Equations 4 and 5, depending on data availability and satellite pairs. Previous study on GSICS GEO-LEO inter-calibration has shown that there is a linear relationship between the GOES radiance and the two reference instruments (Wu et al. 2009). Yet, the slope may be impacted by the radiance distribution of the collocation data. Figure 3 shows the changes of linear regression slopes with the number of homogenous collocation scenes at GOES-11 Imager Ch4. The slopes get stabilized with increasing of collocation data availability. In this study, a minimum of 150 homogeneous scenes are applied to ensure a reliable GEO and LEO relationship.

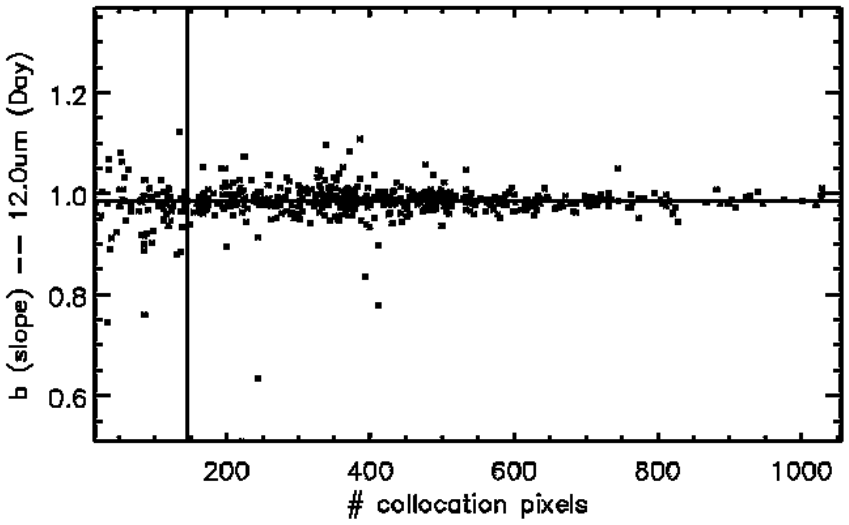

Figure 3. Change of linear regression slopes between homogenously collocated GOES-11 Imager Ch4 and AIRS radiance data.

In this study, Tb bias is defined as the brightness temperature difference between GOES and LEO data ($\Delta Tb = Tb_{geo} - Tb_{leo}$). Since ΔTb is scene temperature dependent, it is also necessary to examine the ΔTb histogram distribution to ensure that the mean ΔTb can represent the collocation data reasonably. Figure 4 shows an example of histogram of ΔTb values of GOES-11 vs. IASI for night-time Ch2 with Gaussian fit distribution. A threshold of chi-square value ($\chi^2 > 1.0$) for the fitting function, which is a goodness-of-fit statistic, is used to further remove skewed Tb biases that may cause an uncertainty in the calibration difference between these two instruments (Wang et al. 2010).

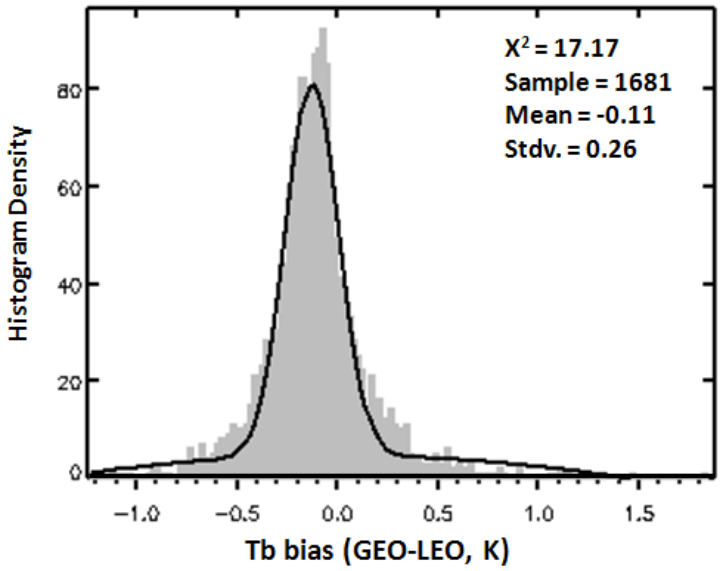

Figure 4. An example of histogram of GOES-11 – IASI Ch2 night-time Tb bias with a Gaussian fit distribution.

Scatter-plots of Tb biases versus viewing conditions show that day-time ΔTb at short-wave channels (Ch2) are still strongly impacted with the bi-directional reflectance distribution (BRDF) effect within the 60^o of relative azimuth angles between the two satellites. A more rigorous azimuth angle alignment threshold may be needed to reduce the BRDF effect. However, a more rigorous relative azimuth angle threshold results in insufficient homogeneous collocation data for further analysis. Therefore, day-time Ch2 collocation data will not be analyzed in this study.

Two periods during which all the radiometer calibrations were relatively stable are used to investigate the diurnal calibration variations within different seasons: January 1, 2008 -March 1, 2008, and from June 1, 2008 - August 1, 2008. The frequencies of MBCC implementation during these study periods are also plotted in the figures. The onset of MBCC status is ingested from the GOES VARiable format (GVAR) data downloaded from NOAA Comprehensive large Array-Data Stewardship System (CLASS). As Aqua crosses the Equator around 1:30am, we use "midnight" to describe the GOES vs. AIRS night-time collocations and "night" for the GOES vs. IASI night-time data. As Aqua AIRS passes the GOES sub-satellite area at these time slots, the AIRS collocated data are used to calculate the diurnal calibration variations, defined as the mean ΔTb around noon (1:00-2:00PM) minus the mean ΔTb around midnight-night (1:00-2:00AM). Data from another stable calibration period from June 1, 2010 to August 15, 2010 are used to examine the GOES scan-angle dependent calibration residuals.

4. Results and Discussions

4.1. Diurnal Variation of GOES Imager Calibration Accuracy

GOES-11 Imager

Channel 2(3.9μm): The consistent and small negative Tb biases to both AIRS and IASI data (<-0.1K, Table 3) indicate that GOES-11 Imager Ch2 is generally well calibrated at night and midnight times. A small but apparent deviation of ΔTb can be observed in winter 2008 after the satellite midnight (Figure 6). MBCC was implemented almost every night during the study period. Since MBCC calibration slopes are calculated from the strong empirical relationship between the daytime operational calibration algorithm slopes derived and the primary telescope mirror temperature (Jackson and Weinreb 1996), the consistent and small Tb bias to these two hyperspectral instruments strongly imply that Ch2 daytime data is also well calibrated.

Channel 3(6.75μm): Seasonal variation of Tb biases to both AIRS and IASI instruments are observed at GOES-11 Ch3. The ΔTb values are larger in summer than in winter (Table 2). Note, though, that the diurnal calibration variations are very similar for these two seasons (~0.2K, Table 3). It was found that these seasonal calibration variations were coincidently with the switches of patch temperature (Wang et al. (2010). This is the only channel that displays apparent seasonal calibration variation in this study. More work will be needed to understand the physical procedure of patch temperature switching and its relationship with changes of calibration accuracy.

The difference between the Tb biases for AIRS and IASI data is very small (<0.1K Table2). The small ΔTb difference confirms that the JMA's gap filling method works successfully in filling the large AIRS spectral gap at this channel as reported by Wang et al. (2010) (Figure 1). As shown in Figures 6 and 7, the MBCC method was implemented with highly frequencies during these two periods. The consistent Tb biases to both LEO instruments exhibits that MBCC works effectively to stabilize the calibration accuracy at night/midnight times. The daytime ΔTb values are larger than those at night/midnight times, indicating that data with the MBCC correction is slightly under-corrected by about 0.2K in this channel (Table 2).

Channel 4(10.7μm): Both satellite pairs show small Tb biases for daytime data (>-0.15K, Table 2). However, this channel has relatively large diurnal calibration variation. The mean diurnal calibration variation is 0.79K in winter and 0.61K in summer (Table 3). As shown in the lower-right panels in Figures 6 and 7, MBCC was frequently implemented after satellite midnight time. Still, no apparent improvement of calibration accuracy can be observed during this period. In fact, there seems to be slight increase of Tb biases after the onset of use of MBCC in the summer 2008. As the MBCC calibration slopes depend on the relationship between day-time calibration slopes and optics temperature, it may be necessary to revisit the empirical relation to improve the midnight calibration accuracy in this channel.

Channel 5 (12.0μm): Large diurnal calibration variation is also observed in this channel. The mean diurnal variation of Tb bias is 0.71K in winter 2008 and 0.50K in summer 2008. This large diurnal Tb biases are due to the insufficient implementation of MBCC correction. As shown in the lower-right panel in Figure 6, MBCC was fully implemented right after the satellite midnight time in winter 2008, coincident with the sudden reduction of Tb bias to AIRS data at the same time. The coincidence indicates that MBCC can reduce the diurnal calibration variation by about 0.4K once fully implemented. Compared to the day-time Tb biases, the MBCC method also slightly under-corrects the midnight data (Ch12.0μm in Figure 6).

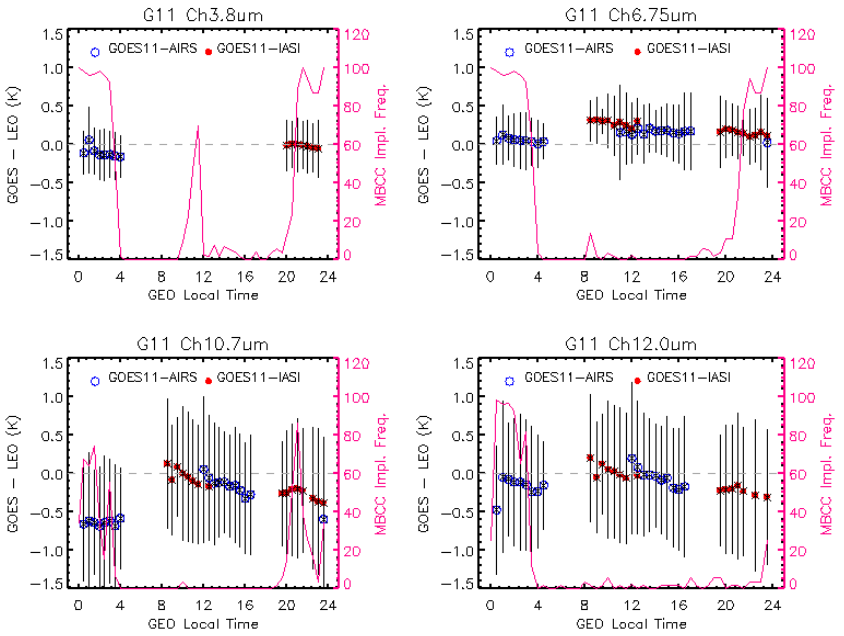

Figure 6. GOES-11 mean Tb bias vs. AIRS (blue circles) and IASI (red circles) in half-hour bins and the standard deviation (black lines) for the collocation data from Jan. 1 2008 – Mar. 1, 2008. The frequency of GOES-11 Imager MBCC implementation on the right-hand second y-axis (labeled in pink).

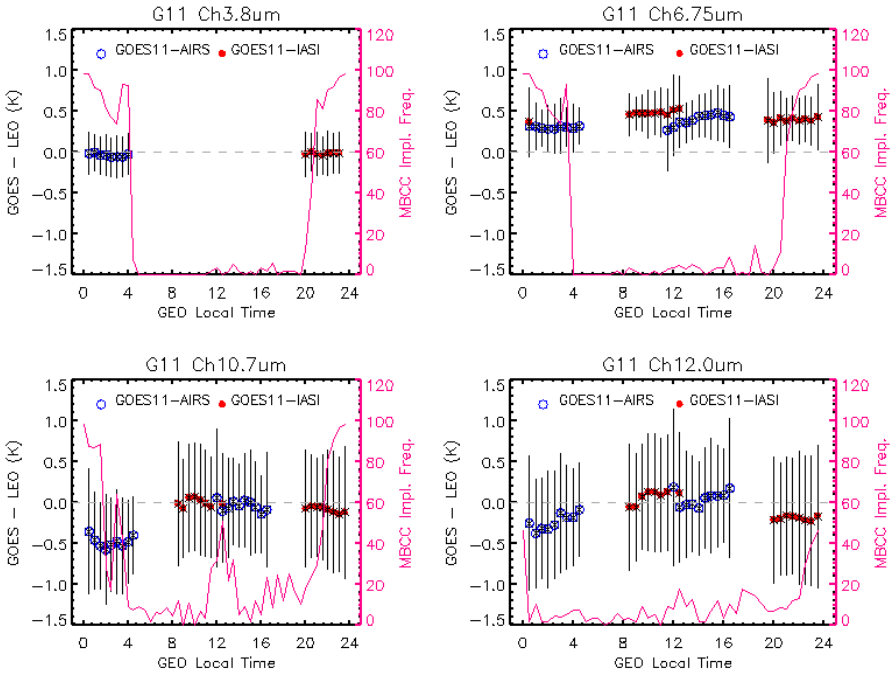

Figure 7. Same as in Figure 6, but for the period of June 1 2008 – August 1, 2008.

GOES-12

Channel 2 (3.9μm): Similarly to GOES-11 Ch2, this short wavelength channel is also well calibrated at night-time with consistent Tb biases (>-0.2K in Table 2, Figures 8 and 9). A similar jump of Tb bias at midnight is also observed in winter time, even after the full implementation of MBCC. The co-occurrence of midnight ΔTb jumps for GOES-11 in winter implies that this calibration anomaly is time dependent, most likely due to stray-light effect at the satellite midnight.

Channel 3 (6.5μm): Day-time data is well calibrated with small variations (<0.20K, Table 3). Again the small difference of ΔTb between AIRS and IASI pairs indicates that the JMA's gap filling method is effective in filling the AIRS spectral gap (Figure 1). Unlike the water vapor channel of GOES-11, there is no apparent seasonal calibration variation at the water vapor channel on GOES-12, probably due to the narrower band-width of the spectral response function (Wang et al. 2010). However, the MBCC was rarely implemented for this channel during the study periods, resulting in continuous progressive changes in Tb biases at night/midnight time. The mean diurnal calibration variations are also relatively large (0.55K in winter and 0.61K in summer, Table 3). The rare implementation of MBCC provides an opportunity to examine the patterns of magnitude and variation of the erroneous instrument responsivity as impacted with the heating instruments. It clearly shows that the calibration error begins about 3-4 hours before satellite midnight time, increases gradually, peaks about one to two hours after midnight, and then reduces gradually. This pattern agrees well with those observed in the ocean surface temperature (Jackson and Weinreb, 1996), but the GSICS data provides detailed independent analysis with higher temporal resolution.

Channel 4 (10.7μm): Similarly to GOES11 Ch4, there is large diurnal calibration variation for this channel. The absolute ΔTb values during daytime are smaller than those at night/midnight times. MBCC was not always implemented during the study periods. However, once implemented, instead of improving the nighttime calibration accuracy, the Tb biases to AIRS data slightly increased, resulting in an increase in the diurnal calibration variation.

Channel 6 (13.3μm): Ch6 has large Tb bias (<-1.K), consistent with the results found by Gunshor et al. (2009) and Wang et al. (2010). Again, the absolute Tb biases are smaller during daytime than nighttime, indicating that day-time data are better calibrated. MBCC was often fully implemented after midnight. However, responses to the onset of MBCC vary by different season. While there was a sudden drop of Tb bias in winter 2008, the Tb biases increased in summer 2008. The MBCC seems to slightly overcorrect the midnight radiance in summer 2008, as the mean Tb biases after full implementation of MBCC was slighter larger than that at noon. However, both jumps adjust the Tb biases closer to the day-time data and thus reduce the calibration variation. As a result, although the maximum diurnal calibration variation is relatively large (0.6 – 0.8K), the difference between mean ΔTb during day and night/midnight times are relatively small for each satellite pairs (<0.3K, Table 2).

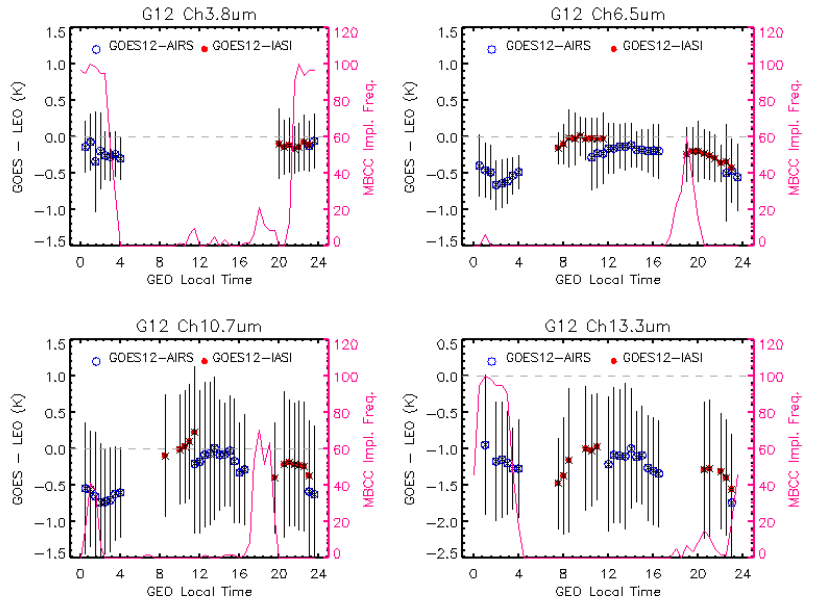

Figure 8. GOES-12 mean Tb bias vs. AIRS (blue circles) and IASI (red circles) in half-hour bins and the standard deviations (black lines) for the collocation data from Jan. 1 2008 – Mar. 1, 2008. The frequency of GOES-11 Imager MBCC implementation during the same period is also plotted on the right-hand y-axis (labeled in pink).

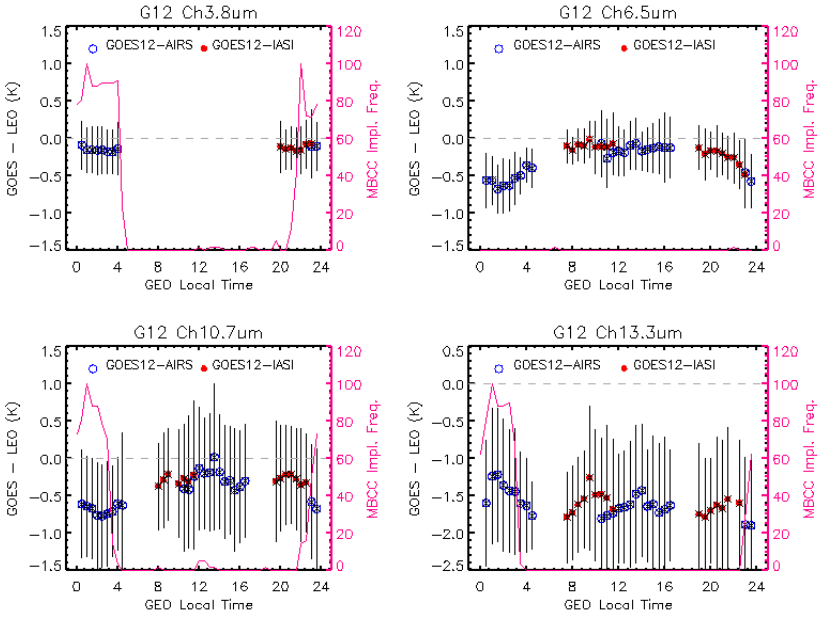

Figure 9. Same as Figure 8 but for the period of June 1 2008 – August 1 2008.

Note that all the long-wave channels have some slight variations in the daytime ΔTb values. As the temperature of GOES calibration related telemetries are stable during day-time (Yu and Wu 2010), these time dependent ΔTb variations should be attributed to the solar/viewing geometric conditions of the collocation data. As previously stated, the GSICS GEO-LEO collocation algorithm applies rigorous viewing zenith alignment thresholds to minimize the optical path difference at large viewing angles. Because the scan-angle effect is very small and negligible (following analysis), the day-time ΔTb variations are most likely caused by the directional emissivity of the Earth, not only over the lands (GOES-12) but also over the surface generally (GOES-11). We applied the same methods to the Spinning Enhanced Visible and Infrared imager (SEVIRI) data from Meteosat-9 which does not have scan angle and midnight calibration anomaly issues. It was found that the night-time collocation data have consistent Tb biases as compared to the AIRS and IASI data, yet there are slight variations in the day-time of the long-wave channels, confirming that daytime collocation may be contaminated with the directional emissivity effect (Wu and Smith 1997).

Table 2. Mean ΔTb to the two hyperspectral instruments during day and night/midnight times for Ch3, Ch4, and Ch5/6. Ch2 has only night-time ΔTb data.

Channel name	Time	**GOES11 - AIRS**		**GOES11 - IASI**	
		Winter	Summer	Winter	Summer
Ch2	Night/ midnight	-0.09(0.33)	-0.03(0.24)	-0.01(0.30)	-0.02(0.26)
Ch3	Day-time	0.18(0.33)	0.42(0.30)	0.29(0.35)	0.47(0.31)
	Night/ midnight	0.06(0.35)	0.30(0.31)	0.14(0.36)	0.39(0.31)
Ch4	Day-time	-0.11(0.76)	-0.02(0.60)	-0.01(0.85)	-0.05(0.85)
	Night/ midnight	-0.64(0.78)	-0.49(0.63)	-0.25(0.90)	-0.08(0.70)
Ch5	Day-time	-0.01(0.80)	0.02(0.66)	0.05(0.89)	0.01(0.88)
	Night/ midnight	-0.15(0.85)	-0.27(0.71)	-0.23(0.92)	-0.19(0.77)

Channel name	time	**GOES12 - AIRS**		**GOES12 - IASI**	
		Winter	Summer	Winter	Summer
Ch2	Night/ midnight	-0.22(0.44)	-0.15(0.32)	-0.12(0.36)	-0.13(0.32)
Ch3	Day-time	-0.16(0.32)	-0.13(0.33)	-0.04(0.33)	-0.10(0.33)
	Night/ midnight	-0.55(0.37)	-0.58(0.37)	-0.31(0.33)	-0.27(0.34)

Ch4	Day-time	-0.10(0.86)	-0.21(0.82)	-0.05(0.87)	-0.32(0.79)
	Night/ midnight	-0.66(0.79)	-0.68(0.71)	-0.25(0.88)	-0.31(0.74)
Ch6	Day-time	-1.13(0.85)	-1.60(0.85)	-1.07(0.96)	-1.54(0.88)
	Night/ midnight	-1.16(0.90)	-1.46(0.90)	-1.34(0.92)	-1.63(0.94)

Table 3. Mean diurnal calibration variation for Ch3, Ch4, and Ch5/Ch6 on GOES-11 and -12, calculated as the mean ΔTb at noon – mean ΔTb values at midnight time for each satellite pairs.

Channel name	**GOES11 - AIRS**		**GOES12 -AIRS**	
	Winter	Summer	Winter	Summer
Ch3	0.20	0.21	0.55	0.61
Ch4	0.79	0.61	0.66	0.64
Ch5/Ch6	0.71	0.50	0.76	0.61

4.2 Calibration Residual of GOES Imager Scan-Mirror Emissivity

The scan angles of the collocation data cover about ±6.0^o for GOES Imagers and about ±40^o for AIRS/IASI instruments. Data used in this study are the homogeneous scenes passing all the selection criteria described in Section 3 from June 10, 2010 – August 15, 2010. To avoid of the effect of anisotropic emissivity, the night time GOES - IASI homogeneous collocation data are used to investigate the scan-angle calibration residuals. In addition, these night-time homogeneous collocation data should occur before 22:00 at satellite local time to minimize the impact of midnight calibration errors. Scan angles east to the meridian longitude of the nadir points are assigned with positive values.

Figures 10 and 11 show the mean ΔTb ($Tb_{goes} - Tb_{iasi}$) and the standard deviations of the homogeneous collocation scenes that fall in each IASI scan angle for GOES-11 and -12, respectively. For each IR channel, the mean ΔTb values are consistent across the large GEO and LEO scan angles with small deviations around the mean values. It seems that GOES-12 has relatively large deviations for scan angles around ±3.5^o in Ch2, Ch4 and Ch6. However, the standard deviation of the mean ΔTb values for each IR channel is less than 0.06K.

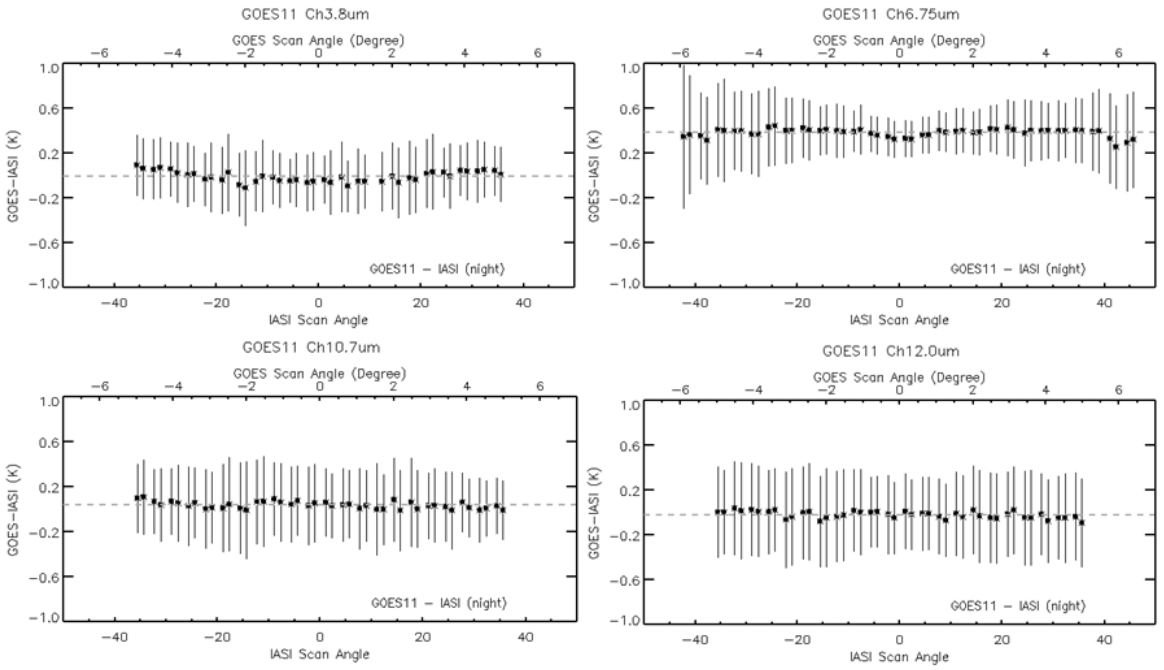

Figure 10. The mean Tb bias to IASI and the standard deviations of the collocation scenes at IASI scan angles for GOES-11. Plotted are only those mean Tb biases at the scan angle which have collocated scenes meeting the minimum collocation number and ΔTb histograms meeting the Gaussian fit requirement. The dashed gray lines are the mean ΔTb bias for each IR channel.

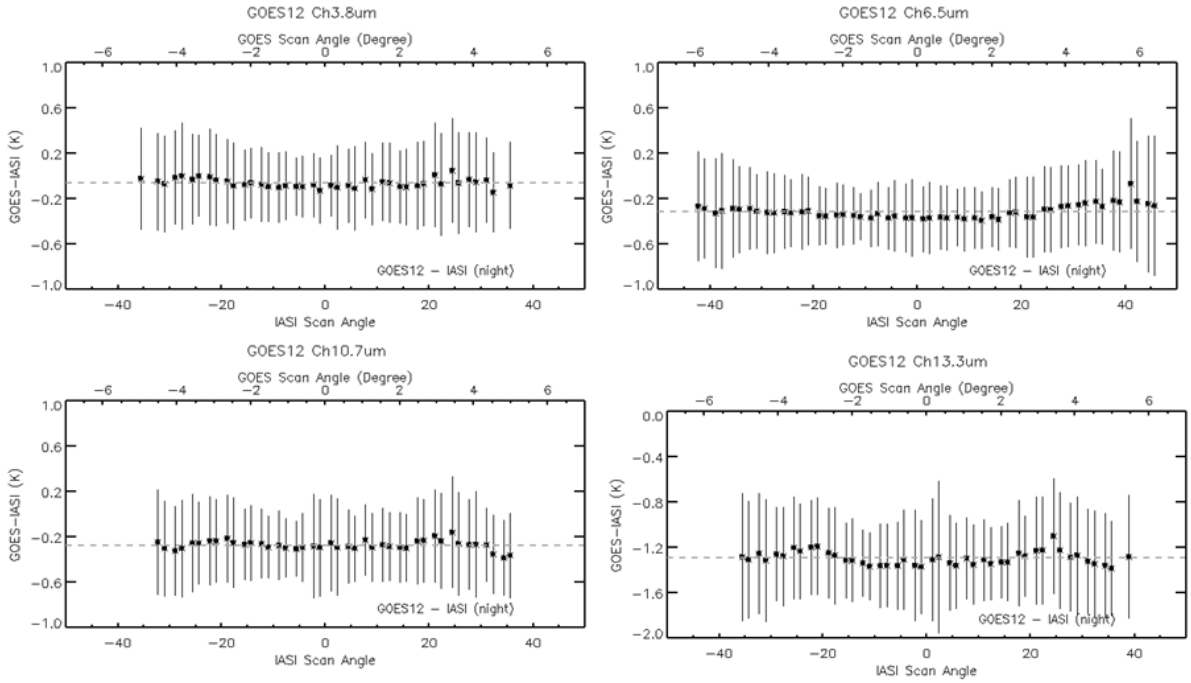

Figure 11. Same as Figure 10 but for GOES-12.

5. Conclusions

In this study, the statistics of homogeneous GSICS collocation data over stable calibration periods are examined for the diurnal and scan angle calibration variations for the IR channels on GOES-11 and -12 Imagers. Due to the strong BRDF effect on the short-wave channels, we do not examine the diurnal calibration variations for these channels. Our results show that data at satellite midnight have the largest Tb biases to the reference instrument for all the IR channels except for Ch3 on GOES-11, which has larger Tb biases in daytime. Diurnal calibration variations exist at Ch3, Ch4, Ch5/6 with the largest values occurring in the long-wave channels. Implementation of the MBCC method helps to reduce the diurnal calibration variation except for Ch4(10.7μm) on both Imager instruments. It is noted that MBCC seems to slightly under-correct the midnight radiance for GOES-11 Ch3 (6.75μm) and Ch5(12.0μm), yet it slightly over-corrects the data for GOES-12 Ch6 in the summer of 2008.

The MBCC method was rarely implemented for GOES-12 Ch3 during the study period, causing about 0.55K-0.61K mean diurnal calibration variations. GOES-11 Ch3 has apparent seasonal calibration variation. Yet, with the fully implemented MBCC interventions, the diurnal calibration variation is consistent at these two seasons, yielding diurnal variations of about 0.2K and indicating the robust relationship of the calibration slopes and the optics temperature at this channel. However, the MBCC method does not improve the midnight calibration accuracy for Ch4 on both GOES instruments. These two channels have 0.6-0.8K diurnal calibration variations. It may be necessary to revisit the empirical relationship used in the MBCC method for this channel.

The wide coverage of the collocation scenes provides us a unique opportunity to examine the GOES scan angle calibration residuals caused by the varying emissivity of the scan mirror. Our analyses indicate that the directional reflectance and emissivity of the collocated scenes exist in daytime collocation data, especially for the long-wave channels of GOES-12. Inter-comparison of GOES - IASI nighttime collocation data indicates there is a very small scan angle dependent calibration residual for each GOES Imager IR channel (<0.1K). Since the day-time collocation data may be affected by directional emissivity, the nighttime GOES vs. IASI collocations two hours before satellite midnight or daytime nadir or near nadir collocations should be used to generate the GSICS GEO-LEO correction coefficients.

Acknowledgements

This work is funded by NOAA STAR calibration and validation, GOES-14 post-launch science test, GOES-R calibration and validation. We would like to thank Dr. Haifeng Qian for his critical review comments on this paper and Mrs Gordana Rancic for the help in processing the historical GOES vs. IASI collocation data. The manuscript contents are solely the opinions of the authors and do not constitute a statement of policy, decision, or position on behalf of NOAA or the U.S. government.

Reference

Aumann, H.H., M.T. Chahine, C. Gautier, M.D. Goldberg, E. Kalnay, L.M. McMillin, H. Revercomb, P.W. Rosenkranz, W.L. Smoth, D.H. Staelin, L.L. Strow, and J. Susskind, 2003. AIRS/AMSU/HSB on the Aqua mission: Design, science objectives, data products and processing systems. IEEE Trans. Geosci. Remote Sensing, 41. 253-264.

Blumstein, D., B. Tournier, F.R. Cayla, T. Phulpin, R. Fjortoft, C. Buil, G. Ponce, 2007. In-flight performance of the infrared atmospheric sounding interferometer (IASI) on Metop-A. *SPIE*, 6604, 66840H-1 (2007), doi:10.1117/12.734162.

Chahine, M. T., and Coauthors, 2006: Improving weather forecasting and providing new data on greenhouse gases. *Bull. Amer. Meteor. Soc.*, **87**, 911–926.

Cao, C., M. Weinreb, and H. Xu, 2004. Predicting simultaneous nadir overpasses among Polar-orbiting meteorological satellites for intersatellite calibration of radiometers. Journal of Atmospheric and Oceanic Technology, 21, 537-542.

Doelling, D., P. Minnis, and L. Nguyen, 2004. Calibration Comparisons between SEVIRO, MODIS and GOES Data. MSG-RAO Workshop, Salzburg, Austria, Sept. 9-10, 20004.

Elloit, D., H. Aumann, L. Strow and S. Hannon, 2009. Two-year comparison of radiances from the Atmospheric Infrared Sounder (AIRS) and the Infrared Atmospheric Sounding Interferometer (IASI). Proc. SPIE, Vol. 7456, 75560S; doi:10.1117/12.826996.

Elloit, D., H. Aumann, S. Broberq, 2010. Comparison of AIRS and IASI collocated radiance for cold scenes, *Proc. SPIE,* Vol. 7807, doi:10.1117/12.860964.

Goldberg, M.D. 2007. Global space-based inter-calibration system (GSICS), *International Society for Optical Engineering (SPIE Proceedings*, Vol. 6684, DOI:10.1117/12.735246.

Hewison, T.J. and M. Konig, 2008. Inter-calibration of Meteosat Imagers and IASI, *Proc. EUMETSAT Satellite Conference*, Darmstadt, Germany, September 2008.

Johnson, R.X. and M. Weinreb, 1996. GOES-8 imager midnight effects and slope correction, *SPIE*. 2812, 596-607.

Minnis, P., A. V. Gambheer, and D. R. Doelling, 2004. Azimuthal anisotropy of longwave and infrared window radiances from CERES TRMM and Terra data. *J. Geophys. Res.*, **109**, D08202, doi:10.1029/2003JD004471.

Mittaz, J. and A. Harris, 2008. Using AATSR as radiance calibration reference for NOAA satellites. *Proc. of the 2nd MERIS/(A)ASTR User Workshop*. Frascati, Italy, September 2008.

Marshall, J. Le, J. Jung and J. Derber. 2006. Improving global analysis and forecasting with AIRS. *Bulletin of the American Metrological Society*, 87, 891-894.

Ohring, G., B. Wielicki, R. Spencer, B. Emery, and R. Datla, 2005. Satellite instrument calibration for measuring global climate change. *Bull. Amer. Meteor. Soc*. 86, 1303-1313.

Pagano, T.S., H.H. Aymann, D.E. Hagan, and K. Overoye, 2003. Prelaunch and In-flight radiometri calibration of the Atmospheric Infrared Sounder (AIRS). *IEEE Trans. Geosci. Remote Sensing*, 41, 265-273.

Parkison, C.L. 2003. Aqua: An Earth-observing satellite mission to examine water and other climate variables. *IEEE Trans. Geosci. Remote Sensing*, 42, 173-183.

Rama Varma Raja, M.K., X. Wu, F. Yu and L. Wang, 2009. Assessment of midnight blackbody calibration correction (MBCC) using the global space-based inter-calibration system (GSICS), *Proc. SPIE*, 456, doi:10.1117/12.825407.

Rama Varma Raja, M.K., X. Wu, F. Yu, L. Wang, and G. Rancic, 2010. A study of night time calibration anomaly in infrared channels of operational GOES-11 and GOES-12 satellites using Global Space based Inter-Calibration System (GSICS). In preparation.

Strow, L.L., S.W. Hannon, M. Weiler, K. Overoye, S.L. Gaiser and H.H. Aumann, 2003. Prelaunch spectral calibration of the Atmospheric Infrared Sounder (AIRS). *IEEEE Trans. Geosci. Remote Sesning*, 41. 274-286.

Strow, L., S. Hannon, D. Tobin and H. Revercomb, 2008. Inter-calibration of the AIRS and IASI operational infrared sensors. *Proceeding 17th Annual Conference on Characterization and Radiometric Calibration for Remote Sensing (CALCON)*, Logan, UT, Utah State University Research Foundation, CD-ROM.

Tobin, D.C., H. Revercomb, F. Nagle, and R. Holz, 2008. Evaluation of IASI and AIRS spectral radiances using simultaneous nadir overpasses. *16th International TOVS Study Conference*, Angra dos Reis, Brazil.

Tahara, Y. and K. Kato, 2008. New spectral compensation method for inter-calibration with high spectral resolution sounder. *Meteorological Satellite Center Technical Note*, 52, Prepared and Distributed by Japanese Meteorological Agency.

Wang, L. C. Cao and M. Goldberg, 2009. Inter-calibration of GOES-11 and GOES-12 water vapor channels with MetOp/IASI. *Journal of Atmospheric and Oceanic Technology*, 26, 1843-1855.

Wang, L., X. Wu, Y. Li, S-H. Sohn, M. Goldberg and C. Cao, 2010. Comparison of AIRS and IASI radiance measurements using GOES Imagers as transfer radiometers. *Journal of Applied Meteorology and Climatology*, 49, 478-492.

Weinreb, M., M. Jamieson, N. Fulton, Y. Chen, J. Johnson, J. Bremer, C. Smith, and J. Baucom, 1997. Operational calibration of Geostationary Operational Environmental Satellite-8 and -9 imagers and sounders. *Applied Optics*, 36(27), 6895-6904.

Weinreb, M. and D. Han, 2003. Implementation of midnight blackbody calibration correction (MBCC). http://www.oso.noaa.gov/goes/goes-calibration/mbcc-implementation.htm

Wu, X. and W. Smith, 1997. Emissivity of rough sea surface for 8-13 μm: modeling and validation. *Appl. Opts*. 36, 1-11.

Wu, X and F. Sun, 2005. Post-launch calibration of GOES Imager visible channel using MODIS, SPIE, 5882, doi:10.1117/12.615401.

Wu, X., T. Hewison, and Y. Tahara, 2009. GSICS GEO-LEO inter-calibration: Baseline algorithm and early results. In Atmospheric and Environmental Remote Sensing Data Processing and Utilization V: Readiness for GEOSS III, Proc. SPIE, 7456, 745604-1-745604-12.

Yu, F., X. Wu, Y. Li, G. Rancic, L. Wang, M.R. Rama Varma Raja, S.H. Song, F. Weng and M. Goldberg, 2009. GSICS GEO-LEO operation at NOAA/NESDIS. In Atmospheric and

Environmental Remote Sensing Data Processing and Utilization V: Readiness for GEOSS III, Proc. SPIE, 7456, 74560A-1-74560A-10.

Yu, F. and X. Wu, 2010. GOES Imager and Sounder instrument performance monitoring system. Calcon, Logan, UT, August 20-24, 2010.